Near-Field Optical Reflective Sensing for Bow Tracking

Laurel S. Pardue
Queen Mary University of London
Mile End Road
London, England
lpls3@eecs.qmul.ac.uk

Andrew P. McPherson
Queen Mary University of London
Mile End Road
London, England
andrewm@eecs.qmul.ac.uk

ABSTRACT

This paper explores the potential of near-field optical reflective sensing for musical instrument gesture capture. Near-field optical sensors are inexpensive, portable and non-intrusive, and their high spatial and temporal resolution makes them ideal for tracking the finer motions of instrumental performance. The paper discusses general optical sensor performance with detailed investigations of three sensor models. An application is presented to violin bow position tracking using reflective sensors mounted on the stick. Bow tracking remains a difficult task, and many existing solutions are expensive, bulky, or offer limited temporal resolution. Initial results indicate that bow position and pressure can be derived from optical measurements of the hair-string distance, and that similar techniques may be used to measure bow tilt.

Keywords

optical sensor, reflectance, LED, photodiode, phototransistor, violin, bow tracking, gesture, near-field sensing

1. INTRODUCTION

Tracking any performer's motions while playing a musical instrument is a challenging task, and this is especially true for violin-family bow technique. Bow tracking has been a frequent topic of research within performing and academic communities, but effective study of live performance requires minimal interference with the performer's normal mode of playing. The ideal tracking system would let the performer use his or her own instrument, require no physical additions or cabling that change its feel, place no restrictions on the performer's motions on stage, yet capture every musically relevant dimension at high spatial and temporal resolution. In practice, every sensor technology will make compromises in one or more of these areas.

Near-field optical reflective sensing holds strong potential for tracking the finer details of performer-instrument interaction. This mode of sensing involves shining a light source, typically an LED, at a reflective object and measuring the intensity of the reflection with a phototransistor or photodiode. The output current is linear with the amount of detected light, which scales approximately with the inverse square of the distance between sensor and object. Several manufacturers produce small inexpensive integrated packages containing both emitter and detector. In contrast to video motion capture techniques, typical distances in near-field optical sensing range from 1-20mm, with the possibility for micrometer-level spatial resolution.

This paper investigates the general performance of optical reflectance sensors and presents an application to violin bow position tracking. Reflectance sensors are attached to the stick of the bow in four locations (Fig. 1) facing towards the hair. The location and pressure of the string against the hair dictates its proximity to the stick at any given point along its length. Analyzing the relative stick-hair distance at several locations is sufficient to determine bow pressure, position, and through position, velocity. The placement of two sensors at the same location but with differing angles should further allow the measurement of tilt.

Bow tracking has been shown to be useful in areas including creative performance [12], studies of bow mechanics [2], and performance analysis [9, 14]. However, since many existing sensor solutions are bulky or expensive, a low-cost, portable system based on near-field optical sensing holds significant potential to broaden access to bow tracking information.

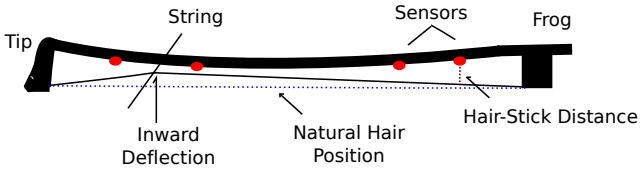

Figure 1: Basic mechanics of hair deformation when the bow is pressed against the string. The string pushes the hair towards the stick. With the two ends of the hair fixed, the resulting hair forms two sides of what we termed the "displacement triangle".

2. PREVIOUS WORK

2.1 Optical Sensing in Musical Contexts

Optical sensing in musical instruments is quite an old idea. Wayne Stahnke used a pair of optical sensors to detect key press and velocity in the original Bösendorfer predecessor to the Disklavier, a design that remains in use today [4]. Middle distance infrared reflectance systems have also been in commercial use for a while with examples such as the Alesis AirFx [17] and the Roland D-Beam [11]. Examples of near-field reflective optical sensors are much more sparse. The Moog Piano Bar, which mounts on top of the piano keyboard, uses near-field reflection off the keys to detect key press [7], while Leroy [5] used them to in an attempt to create an optical pick-up.

NIME'13, May 27 – 30, 2013, KAIST, Daejeon, Korea.

2.2 Bow Tracking

Effective bow gesture capture has been an ongoing target since with Askenfelt's pioneering work in the 1980s. One of the challenges to characterizing bow action is the array of parameters that contribute to the bow-instrument interaction. As identified by Askenfelt and others [1, 13], there are seven main parameters available to a string player when bowing: 1) bow velocity 2) bow pressure 3) bow to bridge distance 4) bow position defined as the transversal position along the bow 5) bow tilt, 6) bow skew defined as the bow's angle to to the bridge and 7) bow attack angle which primarily determines string. The first three are the most important for driving the acoustical response of the string while the remaining four allow the player to effectively control velocity, pressure, and position or add nuance to the tone.

Askenfelt's early work sought to capture bow gesture by altering the bow, adding a thin resistance wire into the bow hair. By also attaching the bow hair to the bow through strain gauges, Askenfelt was able to capture position, pressure and velocity [1]. Askenfelt later was able to capture bow-bridge distance by electrifying the strings to act as resistance wires [2].

Gershenfeld and Paradiso subsequently developed the "Hyper Cello" tracking transversal position and bow-bridge distance through electric field sensing. This was accomplished by attaching an antenna behind a cello bridge to drive a resistive strip along the bow[8]. The hyperbow is an evolution of the "Hyper Cello" and has received many upgrades such as force detection, inertial capture, and wireless operations in the subsequent years[18, 10]. Many of the best practices from the hyperbow have been incorporated into the commercially available K-Bow[1]. A significant drawback of the approach of the hyperbow and K-Bow is the requirement for specialized equipment and the difference in bow feel caused from the technological additions. Schoonderwaldt [15] combined some of the force detection and inertial measurement concepts explored in the hyperbow with camera based optical motion tracking. Although this approach has yielded good bow gesture tracking results, it requires access to a motion tracking system and requires too much post-processing for real-time use.

A significant success towards real-time detailed bow tracking was enabled through electro-magnetic field (EMF) tracking[6]. Maestre used a Pohlemus Liberty[2] EMF tracking system which provides full motion and orientation data. By placing a single small sensor on the bow and a second on the violin, Maestre et al. were able to accurately determine bow transverse position, velocity, and the bow to bridge distance. The approach also enabled the ability to track the string being played and estimate bow pressure. While accurate EMF tracking requires a wired solution and takes non-trivial setup time, the more significant drawback is cost. At over $5000, the Pohlemus and most similar systems are too expensive for general purpose use.

3. NEAR-FIELD OPTICAL REFLECTIVE SENSING

Near-field optical reflective sensors are fairly easy to use qualitatively and to differentiate at the micrometer level, but absolute interpretation of near-field sensing is more of a challenge. There are a number of non-linearities and behavioral characteristics that must be assessed.

3.1 Operational Circuitry

[1] http://www.keithmcmillen.com/k-bow/

[2] http://www.polhemus.com/?page=Motion_Liberty

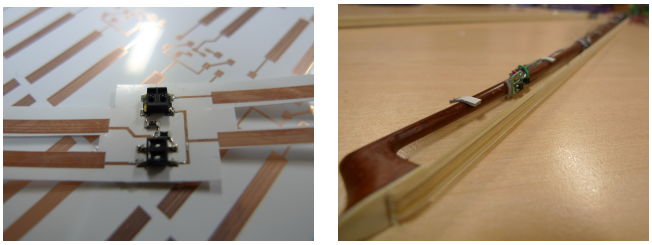

Figure 2: GP2S700HCP and QRE1113 mounted to flex circuit and on test bow.

Near-field optical reflective sensing requires fairly simple circuitry. Fig. 3 outlines the primary two circuit configurations for use with both the photo-transistor and the photo-diode. Current will flow in proportion to the amount of light received at the receiver and this can be measured using a load resistor R_L in either pull-up configuration or with an opamp. Using an opamp marginally increases circuity, but reduces the impedance driven by the transistor output allowing faster operation. In either configuration the principle remains the same: $\Delta V_o = -\Delta I_o R_L$ where I_o is the current output of the photo-transistor and V_o is the measured voltage output. The more current flowing, the lower the measured voltage. The measurable range is otherwise determined by the choice of R_L and the supply voltage.

We investigated three low profile sensors: the Fairchild QRE1113, a reflective proximity sensor with photo-transistor output, the Sharp GP2S700HCP, also a reflective proximity sensor with photo-transistor output, and the Avago HSDL-9100, a proximity sensor with photo-diode output. Compared to photo-diodes like the HSDL-9100, photo-transistors produce more current, but are slower. All three of these sensors are inexpensive and under 2.5mm high. The QRE1113 is 1.7mm high and has an optimal distance range of 1mm. The GP2S700HCP is 2mm high and has an optimal distance range of 3mm. The HSDL-9100 is 2.4mm high with an optimal sense range of 5mm.

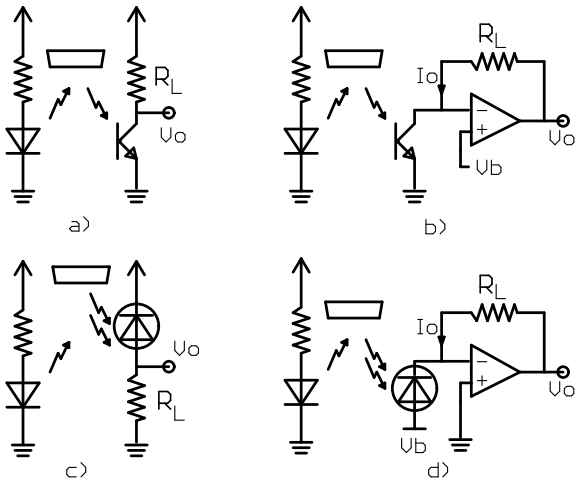

Figure 3: Circuit layouts for using photo-transistors with (a) a pull-up resistor and (b) opamp, or using (c) a photo-diode with a bias resistor or (d) opamp.

3.2 Characterizing Distance Response

One of the key considerations in selecting an optical sensor is its optimal sensing distance and response curve. The horizontal distance between the transmitter and receiver, the transmitter's angular radiation profile, and the receiver's responsivity profile largely determine optimal sensing distance

and the shape of the response curve. As an object comes closer, more of the transmitted light is reflected back a towards the receiver. However, when an object is too close, the region illuminated by the LED will fall outside the sensor's viewing angle as shown in the accompanying graphs. Fig. 4 provides the datasheet sample response curves for both the QRE1113 and the GP2S700HCP. It should be readily apparent that curve is not only irregular, but that due to current drop off below the optimal sensing range, there is potential for ambiguity when interpreting results.

Another major consideration in near-field optical reflectance is the reflectivity of the object being measured. If the object is non-reflective, the current output and range of the photosensor will be dramatically reduced. Bow hair is sufficiently reflective to provide reasonable response.

The third major issue affecting the response curve is the transmitter current. While this does not significantly impact the optimal sensing distance, it will increase the sensing range, lengthening the response curve above the optimal sensing distance.

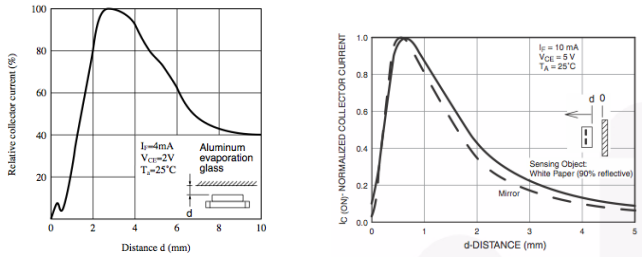

Figure 4: Voltage Output Response Curves for GP2S700HPC (left) and QRE1113 (right). ***Taken from Sharp GP2S700HCP Datasheet, Oct. 2005, and Fairchild QRE1113 Datasheet, Aug. 2011***

Early on it was noticed that different sensors of the same make yielded significantly different current response even when in the same configurations. With the QRE1113 sensors, we have used load resistors ranging between $12k\Omega$ to $47k\Omega$ to achieve similar range. We were even able to notice two physically different manufacturing styles for the QRE1113, each having noticeably different current output. The GP2S700HCP also suffers from this variability between sensors but to a lesser extreme. In a case where the test bow was exposed to an environment where the ambient light significantly overlapped with GP2S700HCP operational frequencies, all GP2S700HCP sensors responded similarly, so we suspect the variation between sensors results from inconsistencies in LED strength.

Because of the variability between sensors, it was useful to determine a sensor's expected performance. A test jig (Fig. 5) has been built for both the QRE1113 and the GP2S700HCP that allows characterization of the sensor output. The jig remains solder free by using compression to force contact with the test circuit pads. Removable acrylic plates enable test heights every 3mm. By testing the sensor before soldering, appropriate load resistance R_L can be selected to match the target operating range and appropriate transmit LED current can be verified.

3.3 Transient Response

In order to test the transient response, each sensor LED was driven using a square wave while tracking the current output in both pull-up resistor and opamp output configurations. The frequency of the square wave was then increased until the output transient failed to settle in time for accurate measurement. In general, when set up in the pull-up configuration, the transistor or diode has to drive a much higher impedance then when the output is configured using an opamp. Higher impedance significantly reduces maximum operational frequency. With a $10k\Omega$ pull-up, the QRE1113 was able to run at 1.4kHz, the GP2S700HCP was able to achieve 2.4kHz. Switching to a $20k\Omega$ pull-up increased response range but slowed the QRE1113 to 400Hz and the GP2S700HCP to 800Hz. Using an op amp configuration, the frequency range was increased to roughly 9kHz for both the QRE1113 and the GP2S700HCP. All tests were conducted driving the sensors with 10mA and the results are consistent with the product datasheets.

According to the product datasheet, the HSDL-9100 has a rise time of only 6 μs, which would enable running at over 150kHz, but that is with a 5.1kΩ load. Unlike the phototransistor, the photo-diode only produces a very small current so that running at 3.3V, a more appropriate load resistance is at least 300kΩ. Driving the sensor LED with 100mA, and a 1M ohm resistor at the output, it was able to run at 5kHz. Switching to an opamp configuration significantly improved the frequency response to 22kHz and possibly higher but it requires significant analog filtering to remove ring and issues from ambient light.

4. PRACTICAL DEMONSTRATION OF BOW TRACKING

The modern violin bow is a tapered and curved wooden stick with tensioned horsehair between the tip and the frog. When the bow hair is pressed against a string, the hair is displaced towards the stick. The amount of displacement at the contact point is determined by the force the bow exerts on the string. As the ends of the hair are fixed, during string contact, the overall hair shape can be described as two sides of a triangle with the maximum displacement at the point of contact with the hair. Because the "displacement triangle" is uniquely determined by both the location of contact and the pressure applied at that contact, it is possible to measure bow transversal position and bow pressure by the stick-hair distance at multiple points along the bow. With accurate bow position it is trivial to derive bow velocity.

We placed eight optical sensors at four locations on the stick of an intermediate level wooden bow selected to maximize expectation of valuable data and distribution across usable space. The approximate locations are represented in Fig.1. The bottom "frog" sensors were placed 75mm from the frog with the "lower" bow sensors an additional 90 mm from the frog. The "tip" sensors were mounted 70mm from the tip with "upper" bow sensors 120mm further down. No sensors were mounted at the extrema as there is little measurable deflection where the hair is secured to the stick, nor did we mount any sensors on roughly the middle third of the stick. During use, there is typically minimal or even no clearance between the hair and stick in the middle section of the bow. A sensor placed too close to the center may not just deform the hair, but far more problematically, clip the string as the sensor moves past.

The clearance issue places a significant constraint on the selection of sensors. If a sensor is too large, it will not be safe to mount places where meaningful data can be collected. It is also necessary to use sensors with a sensing range covering the expected hair-bow distance range.

4.1 Dealing with Non-Linearity and Range

Due to the non-linear curvature of the voltage vs. distance output response curve and its sensitivity to test environment, it is necessary to calculate the output voltage curve empirically. To control for environmental factors, the sen-

sors needed to be tested in the "as used" configuration.

Figure 5: The various test tools (clockwise from rear)- the Razer Hydra and accompanying sensor, scale for future pressure tests with a height jig, height jig used for determining height lookup table, solder-free QRE1113 test jig for sensor evaluation.

For our configuration, the tensioned hair determined our target detection range. Under tension, the hair-stick distance ranged up to 14mm although once mounting and sensor height are taken into account, the needed detection range is reduced to 0 - 11mm. The QRE1113 offers optimal sensing range down to 1mm making it a clear option, however it was not possible choose a R_L that would provide sufficient response above 7mm without saturating the output voltage. The GP2S700HCP has a wider range but empirical tests found current rapidly starts dropping below 2.5mm so many results would be ambiguous. The HSDL-9100 demonstrated detection out to 20mm with an output maxima at 4.5mm. As the QRE1113 is optimal under 4mm, a range overlapping with the GP2S700HCP's optimal range, the combination of the two provides a usable solution.

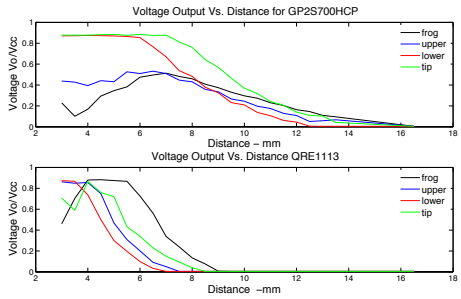

Figure 6: Test Voltage vs. Distance Response Curves for the GP2S700HCP (top) and the QRE1113 mounted on a violin bow.

A voltage vs. distance curve was derived by tests performed using the actual test bow. It was important to test with the actual planned bow setup as bow hair has different width, density, and reflectivity at each end. The QRE1113 and GP2S700HCP were co-located at points along the bow as previously described. A test jig (Fig. 5) was built to separate the hair and the stick at every 0.5mm for distances between 3 and 13.5mm from the stick. Test values taken using the jig were used to build a height lookup table. Fig. 6 illustrates the various voltage vs. distance curves. Results are largely in keeping with the expected curve shapes in Fig.4. An important result is that for each sensor pair, the detection region for the QRE1113 must begin before the peak sensing output of the GP2S700HCP. This is key to resolving the ambiguity introduced by the drop of the response curve after the the peak output.

Using the height lookup table, it is now possible to estimate the displacement heights detected through both senors. We are presently using linear interpolation between data points. By translating the voltage readings to height based on empirical data, we are reducing some of the non-linearities of the optical sensors. With the data now in the same reference frame of *mm*, we can also combine the results from the QRE1113 and the GP2S700HCP into a single distance estimate. At the moment we are using a fairly simple algorithm- if the distance is out of the QRE1113 range, we use the distance measured using the GP2S700HCP. If the GP2S700HCP estimate is higher than the QRE1113, we assume the GP2S700HCP is operating closer than its optimal sensing distance and rely entirely on the QRE1113. If the QRE1113 height is higher than the GP2S700HCP, we take a weighted average. Fig. 7 includes the unified height estimates for a test sample.

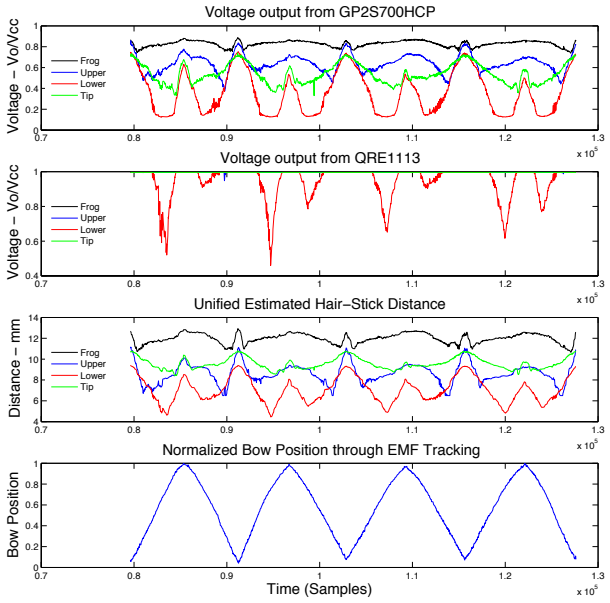

Figure 7: Data taken from a sample test of long bows played from the frog to the tip. From top to bottom: GP2S700HCP voltage, QRE1113 voltage, combined distance measurement, and ground truth bow position as estimated by the Hyrda.

It is worth briefly discussing this intermediate result. Looking at the combined height depicted in Fig. 7, it is easy to visually interpret the data to estimate bow position. At either end of the bow there will be very little overall deflection due to the tension near the anchor points. Starting from the frog, as the bow contact point moves towards the first sensor, the deflection height at that sensor will rapidly drop to its minimum. The estimated bow hair height detected at the other three sensors will also drop but at a slower rates depending on how far they are from the frog. As the string passes the first sensor, that sensor hits its minima and the height to the hair will now increase the farther the bow travels. In the meantime, the second sensor is approaching it's minima and so on. After passing the last sensor at the tip, the measured distance will increase for all sensors as deflection decreases and the next bow stroke back towards the frog begins. Pressure can be estimated by the total scale of the deflection across all sensors.

4.2 Estimating Bow Transversal Position

It is theoretically possible to combine the calculated relative height displacement with a physical model to estimate bow position and pressure. However just as the sensors suffer

from multiple non-linearities, so does the action of the bow. It is not just the hair that deflects, but the bow also bends. Flex and stiffness vary significantly between bows.

We instead decided to use multi-variate polynomial regression to extrapolate position. In our case, the measured bow heights are the four independent variables, and bow position is the conditionally dependent variable for fitting. Since the relationship between the measurements and position should be stable for each sensor arrangement and bow, once we have a polynomial describing that relationship we can use it to extrapolate further bow position.

In order to capture a dependent variable "ground truth", we used the Razer Hydra[3] from Sixense. As an EMF tracking system, tracking using the Hyrda follows the exact same principles as described by Maestre in [6][4].

One EMF tracking sensor was mounted to the tip of the frog while an experienced violinist played a number of bow strokes using the test bow with the optical sensors. At the beginning of each test, the bow was placed at the frog and tip a number of times in order to define the bow's vector of motion. In order to ensure minimal lateral variation, there was a fixed target for right hand extension and the violinst was instructed to stay still. "Ground truth" bow position was derived by translating and rotating the EMF data from the vector of motion onto a single axis (Fig. 7). Tests were run using a variety of stroke pressures to cover the full range of potential hair position.

A convenient result of our approach is that once the polynomial fit is found, it should remain true for a bow provided the same sensors and placements are used. Although the approach does require calibration, it is a one time calibration per bow after which the Hydra is unnecessary.

5. TEST & RESULTS

A sample test result is displayed in Fig. 8. A polynomial transform was determined by using three data sets totaling 7033 samples sampled at 100Hz to fit the four dimensional set of optical sensor heights to normalized bow position. The total number of bow strokes in the fitting set was 29: 15 down bows and 14 up. Each set of data was composed of full tip to frog bow strokes of varying pressure: one set being strong, one being light, and one consisting of bow strokes performed at an in between pressure. The polynomial was then used to estimate bow position based on a data set of hair-stick distances not included in the fitting set. We tested up to a sixth degree polynomial using root mean squared error to evaluate performance.

The sample result set in Fig.8 clearly follows the correct bowing pattern. The test set was 3468 samples long with a RMSE of 0.0635 using a fourth degree polynomial. The raw error was never more that 20%. Expanding the fitting data to include a data set with continuously changing bow pressure reduced the RMSE to 0.051. Similar tests rotating target and training data sets suggested a typical RMSE of between 0.04 and 0.09 and that the fourth order polynomial was generally optimal. These results were all generated prior to any filtering method which would be expected to improve performance. For instance, smoothing results across an 8 sample window reduced the RMSE of the first data set from 0.0635 to 0.0574.

[3]`http://sixense.com/razerhydrapage`

[4]This paper highly recommends a modified Razer Hydra as a poor man's EMF tracking system. It has a more limited range (∼75cm) and less accuracy (∼2mm) than more expensive systems, but at $80, it is dramatically more affordable. The actual sensors are a bit large (20mm) and it is designed as a game controller so that it requires some hacking, but it was sufficient for rough estimate of position.

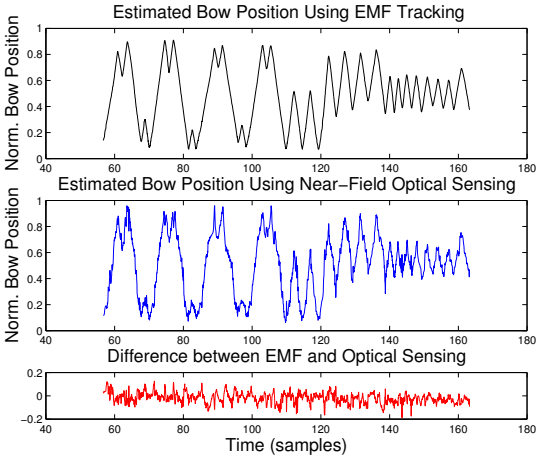

Figure 8: Sample result demonstrating mixed bow strokes. Top: bow position as recorded through EMF tracking. Bottom: estimate of bow position based on near-field optical reflective sensors.

6. DISCUSSION

Our preliminary results using optical senors on the difficult task of bow position tracking demonstrates the potential for near-field optical reflective sensors as a powerful means for fine distance measurement and capturing person-instrument interaction. There remains large scope for improvement through improved build, improved test methodology, addition of sensible filtering, evaluation of additional multi-dimensional fit algorithms, additional data for polynomial fitting and so on. Still, there is obvious initial success to build upon and some of which should be applicable to other sensing contexts.

Bow pressure is a complicated parameter to measure. Part of this is the challenge of measuring pressure in a non-intrusive manner, but part is because players store the bow in an untensioned state, and re-tension the bow each session. The tension also changes during use as the bow reacts to the environment. As tensioning the hair straightens the stick increasing the hair-stick distance, measuring that distance with the bow off the string should give relative tension. Using an approach similar to the one used for position, it should be possible to gather distances at different pressures under different starting tensions to map out pressure characteristics.

The micrometer resolution of near-field optical sensors should also enable the capture of bow tilt. Despite tilt being fairly ubiquitous in playing, with the exception of Schoonderwaldt [16], tilt tracking is fairly neglected. The primary purpose of tilt is to affect tone by controlling the width of hair in contact with the string. Hair in contact with the string will be deflected inward at an angle to the stick while hair not in contact with the string remains largely in its normal tensioned location. Co-locating two sensors, one directed at the hair and one slightly angled, should provide information on tilt based on differences between the two reflectance measurements. Only two sensors are required as string players tilt almost exclusively away from the bridge.

An intriguing immediate result was the clarity with which bow jitter was revealed. Every bow has a point where it will naturally tend to bounce even in a long applied bow stroke. The jitter introduced results in uneven sound, something rarely desirable and whose removal is a common practice target. Similar bounce can happen in an uneven bow change. Optical tracking easily captured this jitter. The software for data collection includes a real-time display of

incoming data. The test violinist was able to see the jitter, data that might otherwise look like noise, and attempt to react to minimize it. While typically aware of jitter, it was informative to have it visually highlighted.

The capture of bow deflection is in itself, a useful result. It seems reasonable that it is possible to derive relative stiffness at different points along the bow as the multiple sensors capture relationships between deflection at these points. Bow deflection characteristics are not directly linked to audible results, but are crucial when considering bow quality and feel for the player.[3]

Cost is also a benefit. The total cost of the sensors outfitted to bow was under $10. Even including the cost of the simple analog conditioning, the supporting processor, and the Hydra, the cost remains under $150. The optical sensors can also be used non-intrusively and there is no obstacle towards optical sensing in a wireless context.

Noise is an issue when using optical sensors. Although the receiver's optimal response frequency is matched to the transmit frequency, it is possible to have interference from the environment. Although all three sensors transmit around a 950nm wavelength, we did not see any evidence of interference between the sensors considered, nor did the QRE1113 react to ambient lighting. Ambient light did not appear to effect the HSDL-9100 either but a small 50Hz frequency in the system power supply became visible in the process of amplifying the μA output. The GP2S700HCP response frequencies did overlap with more common lighting frequencies. Florescent lighting introduced a small 100Hz $50mV$ hum leading to roughly 0.25mm of error. While that error was marginal, the lighting in a studio had such a substantial frequency overlap that it saturated a sensor. As all three types of sensor operate in the IR range, lighting environments emanating substantial IR, such as flash lamps or the Kinect would be expected to interfear. If practical, noise can be dealt with to some degree by directing the sensors away from noise sources, taking a baseline of ambient noise, or increasing transmitter current, allowing a reduction in receiver sensitivity without loss of range. The hum from florescence seen in the GP2S700HCP was sufficiently specific that it should be removable through a notch filter.

7. ONGOING WORK

The use of optical sensors for bow tracking is still in its early stages. As suggested in the discussion, pressure and tilt are two bowing characteristics we intend to investigate. We are also transitioning to a more robust and reliable sensor arrangement. A second hardware version of the system uses flexible circuitry to enable the positioning of two sensors at a reliably fixed distance and offset to each other. This is not only a more reliable setup in general but, as a circuit wraps around the bow, offsetting a sensors from center will result in it being differently angled, enabling tilt investigations.

Another task is to find a non-destructive means for securing the sensors to the bow. They are presently taped to the stick. While effective, easy, and portable, the tape must not damage the bow through left over residue or chemical interaction with the varnish. Finding a suitable tape or other means of securing the sensors will enable use of optical sensors with professional quality bows.

8. CONCLUSION

We have shown that near-field optical reflective sensors can be used to detect one of the major bowing control parameters, position. There is also promise for measuring two other important bowing characteristics, pressure and tilt. Capturing these parameters relies on the excellent spatial and temporal resolution offered by optical sensors. They have further accomplished position tracking in a manner that is non-intrusive to the instrument and minimally intrusive to the player. Lastly, optical sensors offer real-time capable results and are inexpensive.

9. REFERENCES

[1] A. Askenfelt. Measurement of bow motion and bow force in violin playing. *The Journal of the Acoustical Society of America*, 80:1007, 1986.

[2] A. Askenfelt. Measurement of the bowing parameters in violin playing. ii: Bow–bridge distance, dynamic range, and limits of bow force. *The Journal of the Acoustical Society of America*, 86:503, 1989.

[3] A. Askenfelt. Observations on the violin bow and the interaction with the string. In *Proc. of the International Symposium on Musical Acoustics*, 1995.

[4] L. M. Fisher. Ivories that tickle themselves. *The New York Times*, February 1993.

[5] N. Leroy, E. Fléty, and F. Bevilacqua. Reflective optical pickup for violin. In *Proc of New Interfaces for Musical Expression*, pages 204–207, 2006.

[6] E. Maestre, J. Bonada, M. Blaauw, A. Perez, and E. Guaus. Acquisition of violin instrumental gestures using a commercial EMF tracking device. In *Proc. of International Computer Music Conference)*, volume 1, pages 386–393, 2007.

[7] A. McPherson and Y. Kim. Augmenting the acoustic piano with electromagnetic string actuation and continuous key position sensing. In *Proc of New Interfaces for Musical Expression*, 2010.

[8] J. Paradiso and N. Gershenfeld. Musical applications of electric field sensing. *Computer Music Journal*, 21(2):69–89, 1997.

[9] R. Ramirez, A. Perez, S. Kersten, and E. Maestre. Performer identification in celtic violin recordings. In *Proc. of Ninth International Conference on Music Information Retrieval*, pages 483–488, 2008.

[10] N. Rasamimanana, E. Fléty, and F. Bevilacqua. Gesture analysis of violin bow strokes. *Gesture in Human-Computer Interaction and Simulation*, pages 145–155, 2006.

[11] Roland D-Beam. http://www.roland.com/products/en/exp/D_BEAM.html.

[12] E. Rothstein. Yo-Yo Ma and his new 'Hyper' Cello. *The New York Times*, August 1991.

[13] E. Schoonderwaldt. *Mechanics and acoustics of violin bowing: Freedom, constraints and control in performance*. PhD thesis, KTH, 2009.

[14] E. Schoonderwaldt. The player and the bowed string: Coordination of bowing parameters in violin and viola performance. *The Journal of the Acoustical Society of America*, 126:2709, 2009.

[15] E. Schoonderwaldt and M. Demoucron. Extraction of bowing parameters from violin performance combining motion capture and sensors. *The Journal of the Acoustical Society of America*, 126:2695, 2009.

[16] E. Schoonderwaldt, K. Guettler, and A. Askenfelt. Effect of the width of the bow hair on the violin string spectrum. In *Proceedings of the Stockholm Music Acoustics Conference, SMAC*, 2003.

[17] P. White. Review: Alesis Air FX, multi-effects processor. *Sound on Sound*, January 2001.

[18] D. Young. Wireless sensor system for measurement of violin bowing parameters. In *Stockholm Music Acoustics Conference*, pages 111–114. Citeseer, 2003.